# Effect of Floating Water Plants on Wind-Induced Flow in a Closed Water Body

Hamagami, Kunihiko
Laboratory of Bioproduction and Envirnmental Information Sciences,Division of Bioproduction and Envirnment Sciences,Department of Bioproduction Environmental Sciences,Graduate School of Bioresoruce and Bioenvironmental Sciences,Kyushu University

Ozaki, Akinori
Laboratory of Bioproduction and Envirnmental Information Sciences,Division of Bioproduction and Envirnment Sciences,Department of Bioproduction Environmental Sciences,Graduate School of Bioresoruce and Bioenvironmental Sciences,Kyushu University

Mori, Ken
Laboratory of Bioproduction and Environment Information Sciences,Division of Bioproduction and Environment Information Sciences,Department of Bioproduction and Environmental Science,Factory of Agriculture,Kyushu Unviersity

Inoue, Eiji

他

https://doi.org/10.5109/4603

出版情報：九州大学大学院農学研究院紀要. 49 (2), pp.419-431, 2004-10-01. Faculty of Agriculture, Kyushu University
バージョン：
権利関係：

J. Fac. Agr., Kyushu Univ., **49** (2), 419–431 (2004)

# Effect of Floating Water Plants on Wind-Induced Flow in a Closed Water Body

**Kunihiko HAMAGAMI[1], Akinori OZAKI[1], Ken MORI*, Eiji INOUE and Tomokazu HARAGUCHI**

Laboratory of Bioproduction and Environment Information Sciences, Division of Bioproduction and Environment Information Sciences, Department of Bioproduction and Environmental Science, Factory of Agriculture, Kyusyu University, Fukuoka 812–8581, Japan
(*Received June 30, 2004 and accepted July 13, 2004*)

In some closed water bodies with little inflow and outflow, a flow is loose. So it has the different hydraulic characteristics from a river or an irrigation canal. When there is no disturbance, fluid is stratified based on vertical density distribution. In these bodies, the main dynamics of the water environmental substance depends on a mechanical disturbance, which is induced by the wind current on the water surface, and a thermal disturbance, which is induced by convective flow. We especially considered the mechanical disturbance based on the wind-induced flow. The previous study, which studied about the closed water body with floating water plants reported that the existence of the floating water plants may shorten the fetch and affect the dynamics of a density interface. Thereat in our study, we experimentally studied the relationship between the gregarious density of the floating water plants and the wind-induced flow in the closed water body. The result indicated that when the gregarious density of the floating water plants on the water surface becomes small, the values of the turbulent characteristics variables in the upper layer increase. This study clarified that vegetation density affects the entrainment phenomenon in a stratified water body.

## INTRODUCTION

When there is no disturbance in some closed water bodies with little inflow and outflow, fluids are stratified based on vertical density differences with temperature, substance concentration, and the other density differences. Therefore, the heat and the substance are conveyed by the only density current. In the river, water is always flowing, so even if a pollutant flows in it, the concentration of a pollutant decreases with time. But inflow is little in the closed water body, and the self-purification is scarce compared with a river. So it is easy to generate eutrophication or water pollution. Recently, the concern about an environmental problem is increasing, and the closed water body where especially eutrophication has been serious has been studied in various fields of research.

In the recent study, it was reported that the aquatic plants which live around a water area have the capability which absorbs the nutrients salts leading to eutrophication. And the technique of the water quality purification with the aquatic plants was proposed. On the other hand, since there are little inflow and outflow in the closed water body, the

[1] Laboratory of Bioproduction and Environmental Information Sciences, Division of Bioproduction and Environment Sciences, Department of Bioproduction Environmental Sciences, Graduate School of Bioresource and Bioenvironmental Sciences, Kyushu University

* Corresponding author (E-mail: moriken@bpes.Kyushu-u.ac.jp)

main factors of the behavior for the water environmental substance are mechanical disturbance, which based on the wind–induced flow, and thermal disturbance, which based on the convective flow. The wind current on the water surface of a closed water body with density stratification gives rise to the entrainment phenomenon at the density interface, and it lowers the density interface and increases the density of the upper layer. The fluid mixture between the upper and lower layers based on the entrainment phenomenon significantly influences the water quality of the water body.

The internal circulation based on the mechanical or thermal disturbances in a closed density stratified water body have been studied in the 1980s with the advancement for water supplies, and the rise of the concern about an environmental problem (Mori *et al.*, 1989).

In the closed water body with floating water plants, these plants shorten the fetch, and affect the entrainment phenomenon at the density interface and turbulent structure on the density interface based on the wind–induced flow. In previous studies, it was reported that when floating water plants grew to the water surface of a closed water body, the entrainment velocity decreased as the coverage increased. This is because the existence of the plants decreases the amount of turbulent flow energy produced based on the wind–induced flow and then reduces the capability of the vertical mixture (Ozaki *et al.*, 2002).

However, these studies considered the floating water plants with a comparatively large leaf area, but not about the floating water plants with a small leaf area which moved independently by the water surface wave. Then, this study especially considered the floating water plants with a small leaf area which grew gregariously in the water body, and investigated the entrainment phenomenon at the density interface and the turbulent structure on the density interface.

## METHODS AND RESULTS

### Hydraulic experiments on the entrainment phenomenon

*Experiment equipment*

The test tank consisted of an acrylic plate (length 6 m × width 0.3 m × depth 0.4 m).

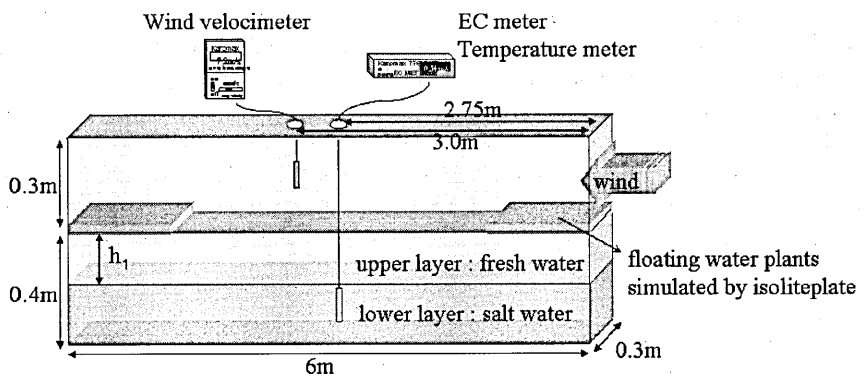


**Fig. 1.** Experimental equipment.

The wind tunnel consisted of a piece of block board on the test tank (length 6 m × width 0.3 m × depth 0.3 m) (cf. Fig. 1). A two-layered stratified density flow is made in the test tank. The upper layer is fresh water and the lower layer is salt water. We experimented on the entrainment phenomenon at the density interface based on the wind-induced flow by use of this equipment. The salinity was measured with a conductance meter, the wind velocity with a hot-wire velocimeter, and the water temperature with a thermocouple. Salinity and water temperature ware measured at 2.75 m from the windward end, and Wind velocity was at 3 m.

*Simulated method of the floating water plants*

Instead of using real floating water plants we used simulated floating water plants made from polystyrene form plates. And the structure of the floating water plants community was simulated by making them a 4-division (cf. Fig. 2 (b)) or a 9-division (cf. Fig. 2 (c)). When the number of division increased, it simulated decreasing of the gregarious density of the floating water plants. We set them at both ends of the test tank. This is because that the floating water plants are distributed from the circumference part like concentric circle-wise toward the center of the closed water bodies.

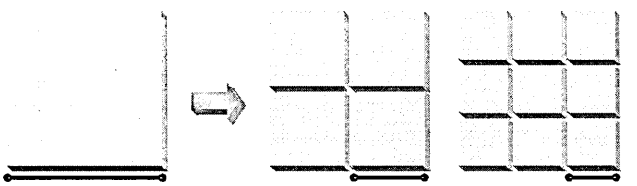


**Fig. 2.** Simulated floating water plants.

*Experimental method*

The experiment was run on the condition that the over all Richardson number $R_{ia}$(= $\Delta\rho_0 g h_{10}/\rho_a u_{*a}^2$) is under 100 for various cases of the simulated objects. In the $R_{ia}$, $\Delta\rho_0$ is the difference of density between the upper and lower layers; $h_{10}$ is the initial water depth of the upper layer; and $u_{*a}$ is the air friction speed. The experimental conditions are shown in Table 1. The measured parameters are the vertical profiles of wind velocity, the water temperature and the salinity.

*Representative wind velocity and Air friction speed*

Fig. 3 shows the measurement results of a wind velocity distribution measured at 2.75 meters from the windward end. The air friction speed is $u_{*a}$ defined by use of distribution of water surface wind complying with logarithmic law as the following equation.

$$U/u_{*a}=(1/\kappa)\ln(z/z_0), \tag{1}$$

**Table 1.** Experimental conditions for entrainment phenomenon.

| Run No. | Coverd Rate (%) | Wind velocity Average (m/s) | $\Delta\rho \times 10^3$ (kg/m$^3$) | $\rho_a$(kg/m$^3$) | $h_i$(m) | $u_{*a}$ (m/s) | $R_{ia}$ |
|---|---|---|---|---|---|---|---|
| RUN I–1 | 10 | 5.4 | 0.0068 | 0.00121 | 0.096 | 25.37 | 81.72 |
| RUN I–2 | 10 | 5.6 | 0.0040 | 0.00122 | 0.106 | 26.05 | 50.05 |
| RUN I–3 | 10 | 5.7 | 0.0020 | 0.00121 | 0.108 | 27.13 | 24.08 |
| RUN I–4 | 10 | 5.7 | 0.0079 | 0.00123 | 0.116 | 27.27 | 97.83 |
| RUN I–5 | 10 | 5.7 | 0.0047 | 0.00123 | 0.110 | 27.22 | 55.89 |
| RUN I–6 | 10 | 5.7 | 0.0039 | 0.00123 | 0.106 | 26.88 | 45.40 |
| RUN I–7 | 10 | 5.5 | 0.0028 | 0.00123 | 0.106 | 25.43 | 36.40 |
| RUN II–1 | 10 | 5.5 | 0.0096 | 0.00126 | 0.096 | 25.74 | 108.06 |
| RUN II–2 | 10 | 5.5 | 0.0062 | 0.00126 | 0.096 | 25.64 | 70.27 |
| RUN II–3 | 10 | 5.6 | 0.0083 | 0.00125 | 0.106 | 26.63 | 97.41 |
| RUN II–4 | 10 | 5.6 | 0.0062 | 0.00126 | 0.116 | 26.61 | 78.74 |
| RUN II–5 | 10 | 5.5 | 0.0034 | 0.00125 | 0.096 | 25.74 | 38.74 |
| RUN II–6 | 10 | 5.7 | 0.0025 | 0.00125 | 0.106 | 26.99 | 28.38 |

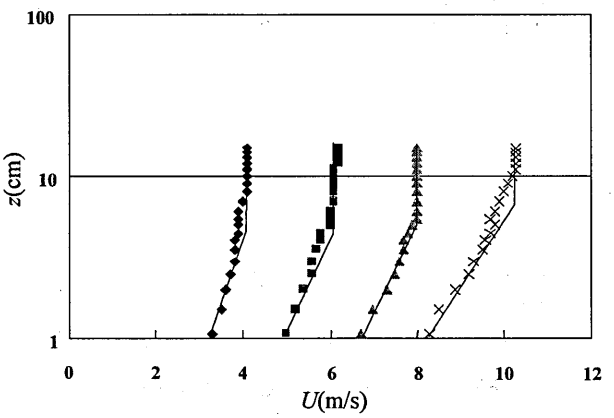


**Fig. 3.** Wind velocity distribution measured at 2.75 m from the windward end.

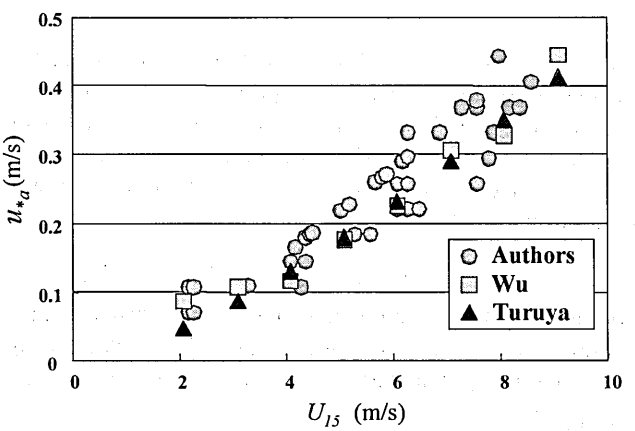


**Fig. 4.** Relation between the air friction velocity and the wind velocity.

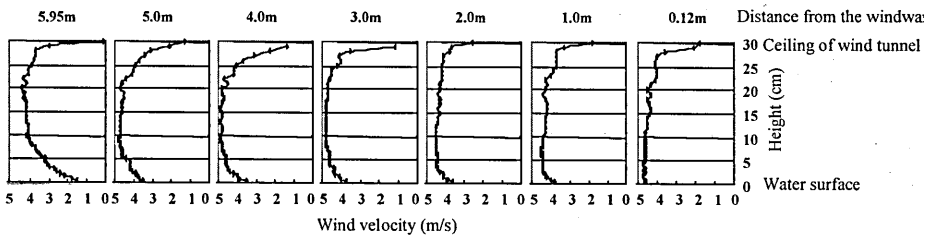


**Fig. 5.** The characteristics of the wind tunnel.

where $U$ is the wind velocity at height $z$; $z$ is the height from the water surface; $\kappa$ is the Karman constant; and $z_0$ is the roughness constant. The hatched solid line drawn on Fig. 3 is the regression line. Fig. 4 shows the relation between the air friction speed $u_{*a}$ obtained by the above equation and the wind velocity at 0.15 m above the water surface. This figure includes the experimental results in previous studies (Wu, 1973; Tsuruya, 1983). Fig. 5 shows the characteristics of the wind tunnel used in this experiment. Although it is influenced of the ceiling in the upper part of the wind tunnel, the logarithmic law is approved near the water surface.

*Coefficient of entrainment and overall Richardson number*

The scale of entrainment velocity is generally given by the coefficient of entrainment $E$ and the overall Richardson number $R_{io}$, which are defined as

$$E=\frac{u_e}{V}$$

$$R_{io}=\frac{\Delta\rho g h}{\rho V^2} \tag{2}$$

where $u_e$ is the entrainment velocity; $V$ is the reference velocity of flow; $h$ is the water depth of the upper layer; $\rho$ is the reference density; $\Delta\rho$ is the density difference between the upper and lower layers; and $g$ is the gravitational acceleration.

On condition that the water flow is two-dimensional and the section of flowing water under consideration is rectangular, the continuity equation of the flow rate and the density conservation law for the upper layer are respectively given as

$$\frac{\partial h_1}{\partial t}+\frac{\partial(u_1 h_1)}{\partial x}=u_e \tag{3}$$

$$\frac{\partial(\rho_1 h_1)}{\partial t}+\frac{\partial(\rho_1 u_1 h_1)}{\partial x}=\rho_2 u_e \tag{4}$$

where $u_1$ is the cross-average velocity of the upper layer; $h_1$ is the upper water depth; $\rho_1$ is the density of the upper layer; $\rho_2$ is the density of the lower layer; $x$ is the mainstream direction; and $t$ is time. In wind-induced flow, the second term of the left-hand side member of Eq. (3) is small. Hence the entrainment velocity is able to represent the rate of variation of the upper water depth with time, i.e., the descending velocity of the den-

sity interface, as shown below.

$$\frac{dh_1}{dt} = u_e \tag{5}$$

Eq. (3), by Eq (4) and $\Delta\rho = \rho_2 - \rho_1$,
yields

$$\frac{\partial \rho_1}{\partial t} + u_1 \frac{\partial \rho_1}{\partial x} = \frac{\Delta\rho}{h_1} u_e \tag{6}$$

On the condition that lower water entrained to the upper layer is rapidly and uniformly mixed and diffused in the vertical and horizontal directions, Eq. (6) yields

$$\frac{d\rho_1}{dt} = u_e \frac{\Delta\rho}{h_1} \tag{7}$$

By performing integration under the condition that $\rho_2$ is constant, we obtain the following from Eq. (5) and Eq. (7),

$$h_1 \Delta\rho = h_{10} \Delta\rho_0 = const. \tag{8}$$

where $h_{10}$ is the initial upper water depth and $\Delta\rho_0$ is the initial difference of density between the upper and lower layer. Hence we can substitute as follows:

$$H \rightarrow h_{10},\ \Delta\rho \rightarrow \Delta\rho_0,\ \rho \rightarrow \rho_a,\ V \rightarrow u_{*a},$$

where $u_{*a}$ is the air share velocity; and $\rho_a$ is the air density.
Thus Eq. (2) can be described below as a time–invariant equation

$$R_{ia} = \frac{\Delta\rho_0 g h_{10}}{\rho_a u_{*a}^2} \tag{9}$$

and, by Eq. (5), the coefficient of entrainment $E$ can be described as

$$E = \frac{dh_1/dt}{u_{*a}} = \frac{u_e}{u_{*a}} \tag{10}$$

*Experimental results*

Fig. 6 shows variation of the upper water depth based on the wind–induced flow with time. The vertical axis shows the amount of reduction of the density interface $\Delta h (= h_{1t} - h_{10})$, where $h_{1t}$ is the upper water depth at time t, and a horizontal axis shows lapsed time. Although the variation was large for a while after the wind current because of formation of a circulation flow and development of an internal wave, it became linear with time. Since a previous experiment without floating water plants (Mori *et al.*, 1989) shows the same tendency, we can conclude that the lowering of the velocity of the density interface is constant except shortly after running.

About the entrainment velocity at the density interface based on the wind–induced flow with floating water plants, it also turns out that the entrainment velocity is $u_e = dh_1/dt = const$ like a previous study without floating water plants. The entrainment velocity obtained in this experiment is made dimensionless with the air friction speed, and it was defined as entrainment coefficient. Fig. 7 shows the relation between the entrain-

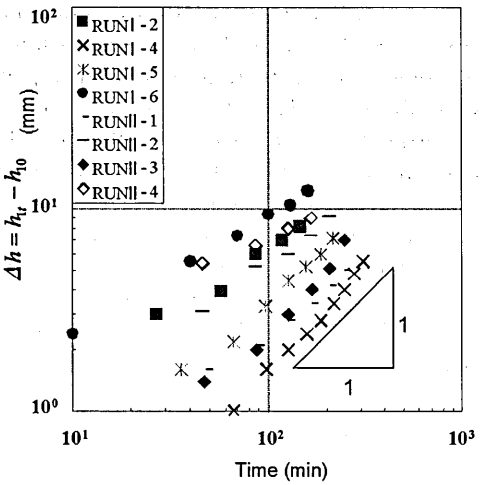


**Fig. 6.** Variation of interface slope with time for various over all Richardoson number.

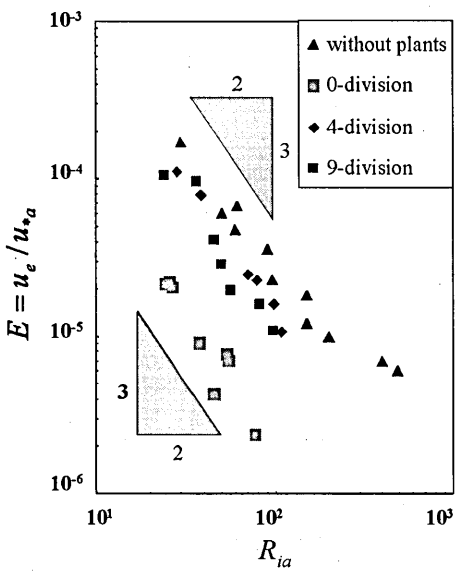


**Fig. 7.** Entrainment coefficient $E=u_e/u_{*a}$ plotted logarithmically as a function of overall Richardoson number $R_{ia}$.

ment coefficient and the overall Richardson number. The previous study defined $E \propto R_{ia}^{-3/2}$ in $R_{ia} < 100$. In this figure, the triangle mark ▲ shows the experimental result without floating water plants in the study of Mori *et al.* (1989), and the quadrangle mark □ shows the experimental result with floating water plants of 10% of covered rate in the

study of Ozaki *et al.* (2002). From this figure, it also turns out that the relation of $E \propto R_{ia}^{-3/2}$ in $R_{ia} < 100$ is mostly satisfied the result of the previous studies. Moreover, it turns out that the entrainment velocity with divided simulated object is larger than with simulated object which is not divided, and smaller than without plants. However, there is almost no difference in the entrainment velocity by the difference of division pattern.

Fig. 8 shows that the coefficient of proportion $k_\beta$ defined by $E = k_\beta R_{ia}^{-3/2}$, where $\beta$ means the number of division of the simulated object. The scale of the vertical mixture by the difference of the number of division of the simulated object is able to estimate from Fig. 8. When the value of $k_\beta$ without plants defines as 100%, the 9–division is 38%, the 4–division is 48% and the 0–division is 7%. Although the value of the divided simulated objects becomes low compared with it without plants, the difference between the 9–division and the 4–division is not clearly.

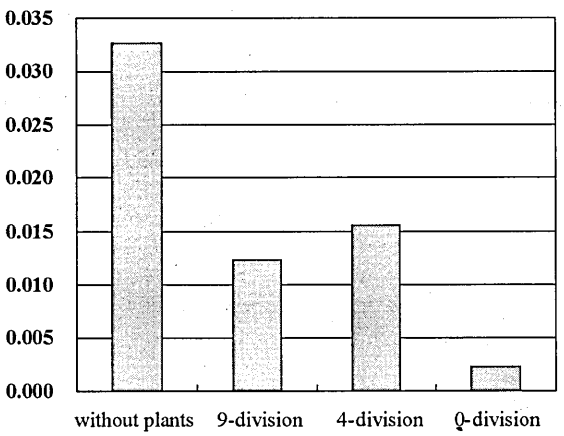


**Fig. 8.** Experimental data for $k_\beta$ as a function of $\beta$.

## Hydraulics experiment of the turbulent structure in the upper layer

*Experimental method*

The equipment and methods for this experiment were the same as for the entrainment phenomenon. The experiment conditions are shown in Table 2. The measured parameters are the profiles of the flow velocity, the water temperature and the salinity. The flow velocity was measured with an X–type hot–wire velocimeter, the salinity was with a conductance meter, and the wind velocity with a hot–wire velocimeter. Measurement points were at 3 m from the windward end of the tank i.e., the center of the tank (named Point A), and at 5.6 m i.e., the edge of the floating water plants (named Point B). The sampling time and the sampling point interval of the horizontal flow velocity $u$, the vertical flow velocity $v$, and the density variation $\rho$ are shown in Table 3. Since it is thought that the density variation near the density interface is greatly influenced of the internal wave, the sampling time near the density interface was set for 60

**Table 2.** Experimental conditions for turbulent structure.

| measurement point | simulated object | Wind velocity $U$ (m/s) | $h_1$ (cm) | $\Delta\rho$ (kg/m$^3$) | $\rho_a\times10^3$ (kg/m$^3$) | $u_{*a}$ (cm/s) | $R_{ia}$ | $u_*$ (cm/s) |
|---|---|---|---|---|---|---|---|---|
| PointA | without plants | 4.7 | 10.8 | 0.00523 | 0.00126 | 20.748 | 102.35 | 0.735 |
| | 0–division | 4.8 | 10.1 | 0.00552 | 0.00126 | 21.372 | 94.85 | 0.759 |
| | 4–division | 4.8 | 11.0 | 0.00554 | 0.00127 | 21.372 | 102.63 | 0.763 |
| | 9–division | 4.8 | 11.0 | 0.00546 | 0.00126 | 21.372 | 102.41 | 0.758 |
| PointB | without plants | 4.8 | 11.6 | 0.00552 | 0.00127 | 21.372 | 107.86 | 0.763 |
| | 0–division | 4.8 | 11.0 | 0.00536 | 0.00128 | 21.372 | 99.15 | 0.764 |
| | 4–division | 4.8 | 11.0 | 0.00554 | 0.00127 | 21.372 | 102.63 | 0.763 |
| | 9–division | 4.8 | 11.0 | 0.00544 | 0.00127 | 21.372 | 100.88 | 0.763 |

**Table 3.** Sampling time and sampling point interval.

| height from the density interface (cm) | sampling time (s) | sampling point interval (cm) |
|---|---|---|
| 0~3 | 60 | 0.5 |
| 3~5 | 25 | 0.5 |
| 5~10 | 25 | 1 |

seconds and the sampling frequency was set to 100 Hz in consideration of the cycle of the internal wave. From the obtained data, we calculated the horizontal and vertical flow velocity, the horizontal and vertical turbulent intensity, the turbulent intensity of density, the Reynolds stress, and the vertical flux. The upper turbulent flow structure has been quantitatively investigated with them.

*Experimental results*

Fig. 9 shows the profiles of the time average flow velocity in the horizontal and vertical directions. The horizontal and vertical axes are made dimensionless with the friction speed and the upper water depth. In the figure, the wind direction is from the right to the left. $z/h_1=1$ represents the water surface and $z/h_1=0$ represents the density interface. The horizontal flow was swept leeward by the wind–induced flow near the water surface (wind–driven current). The magnitude of velocity decreases from the water surface to the density interface, and the flow direction reverses at about 40 percent of the upper water depth from the water surface (return current). That is, it turns out that the vertical circulation flow arises in the test tank. The position of the shift point from the wind–driven current to the return current moves upward as the velocity near the water surface become small. This results showed the same tendency both the Point A and Point B.

The horizontal flow velocity with simulated objects was low compared with the horizontal flow velocity without plants at the Point A. However, there was little difference by dividing the simulated objects. On the other hand, the horizontal flow velocity increased by dividing the simulated objects at the Point B.

The vertical flow velocity defines the upward flow which goes from the density interface to the water surface as positive. At the Point A, the flow direction becomes downward near the water surface. Its velocity decreases as the measurement point approaches

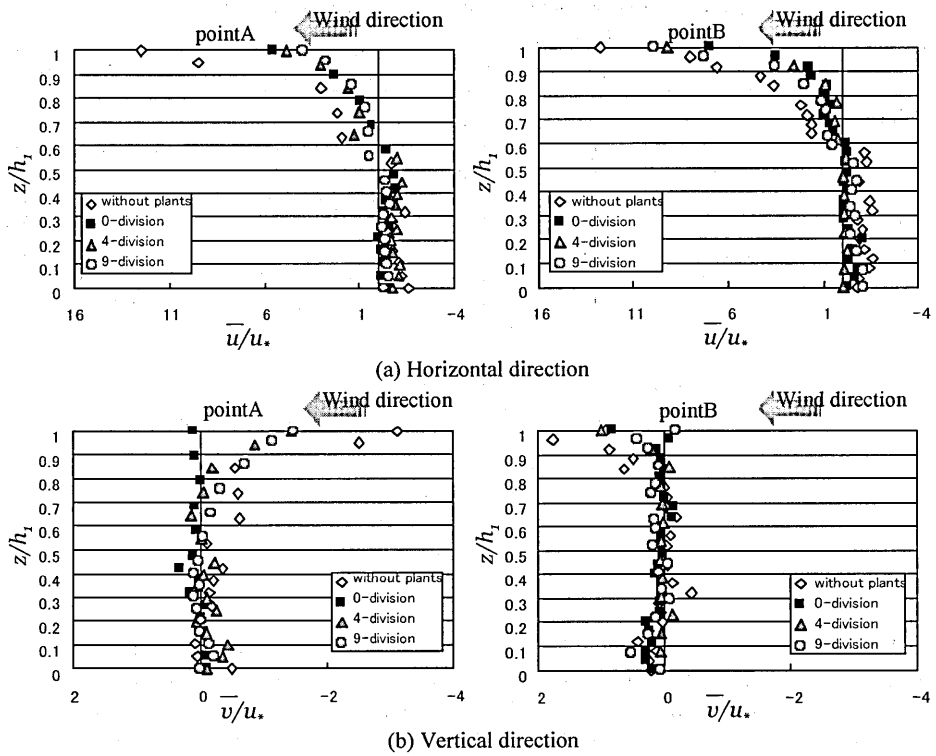


**Fig. 9.** The profiles of time average flow velocity in the horizontal and vertical directions.

the density interface, and it became almost zero uniformly under the position of about 50 percent of the upper water depth. The vertical flow velocity was the largest in the case without plants and tended to decrease as the number of division of simulated objects became few. On the other hand, at The Point B, although it scattered widely within the range of a positive value near the water surface, we could not clarify the variation of it by difference of division pattern. Near the water surface, the profiles of the vertical flow velocity without simulated objects were scattered most broadly, but with the 0-division simulated objects were least. Moreover, the more the number of division of the simulated objects increase, the more the profiles were scattered.

Fig. 10 shows the profiles of the time average turbulent intensity in the horizontal and vertical directions. Both the Point A and Point B, the turbulent intensity in the horizontal and vertical directions are the largest near the water surface, and decrease to the almost same value to about 30 percent of the upper water depth. There was no influence by the division pattern at the Point A. On the other hand, the more the number of division of the simulated objects increase, the more the value of the turbulent intensity increased at the Point B.

At the Point A, the division pattern of the simulated objects doesn't affect the time

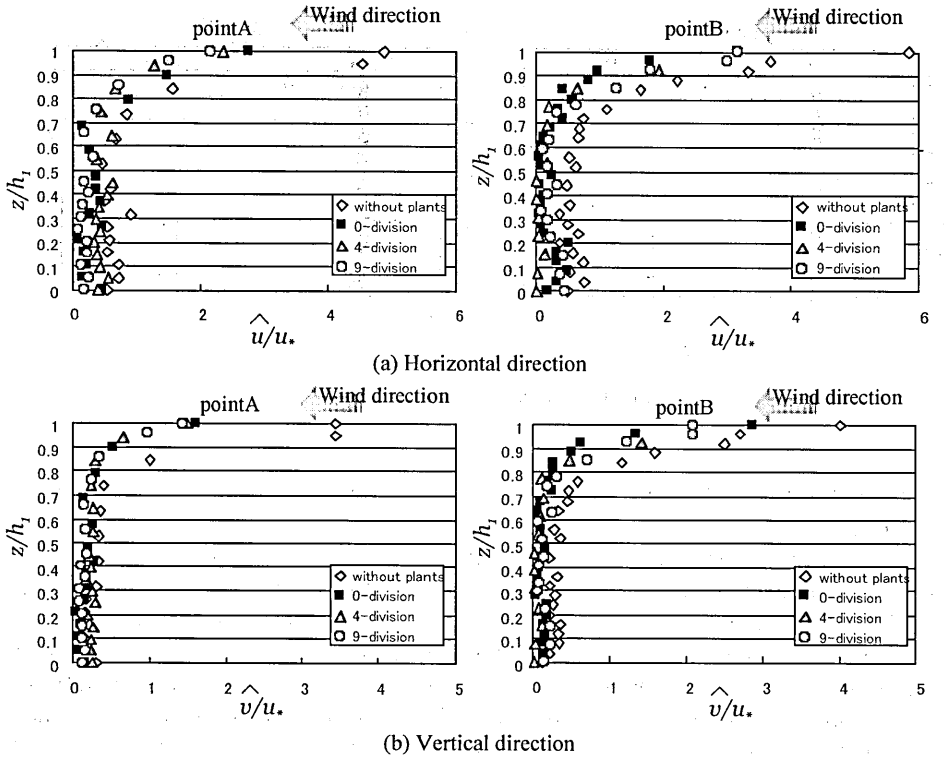


**Fig. 10.** The profiles of time average turbulent intensity in the horizontal and vertical directions.

average flow velocity and the turbulent intensity. This is guessed by the following reason. Generally, the water surface wave in the wind–induced flow is formed from the windward side and develops as it propagates to the lee. The simulated object set at the windward has not effect on the water surface wave without regard to any number of divisions. On the other hand, at the Point B, the more the number of division of the simulated objects increase, the more magnitude of the flow velocity and the turbulent intensity become large. That is, since the water surface wave is completely developed leeward (Tsuruya, 1983), the energy which a water surface wave moves simulated objects. And if the simulated objects were divided, each move independently. Therefore, the more the number of division of the simulated objects increase, the more influence given to the flow velocity and the turbulent intensity increase. In order to examine such a mechanism in detail, it is required to increase the number of division of the simulated objects and to verify the difference of the water surface wave.

Fig. 11 shows the profiles of the Reynolds stress. The Reynolds stress shows the generation source of turbulence. On every condition, it was large only near the water surface, and it became zero mostly to about 20 percent of the upper water depth. This means that production of turbulence originates in the shearing force on the water surface,

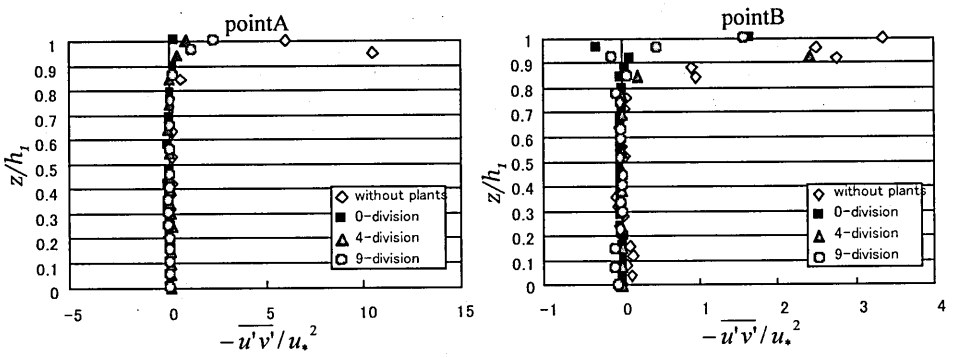


**Fig. 11.** The profiles of the Reynolds stress.

and that the turbulence has taken place into a water body by transporting the energy to the lower part.

Fig. 12 shows the profiles of the density flux. The flux represents transportation of the substance in near the density interface, i.e., a mixed scale. It was large only near the density interface. Therefore, it turns out that fluid exchange based on the turbulent flow between the upper and lower layers is performed in the density interface. Compared among the values near the density interface at the Point A, the case without plants was the largest, and in another cases, it was mostly the about 50 percent of the case without plants. The scale of vertical mixture at the Point B was small compared with the Point A, and the more the number of division of the simulated objects increase, the more the value were large the same as the flow velocity distribution. Thereby, it turns out that the vertical mixture between the upper and lower layers is taken place more strongly at the Point A of the center of the tank, and that the variation by the difference of the number of division appears more notably at the Point B.

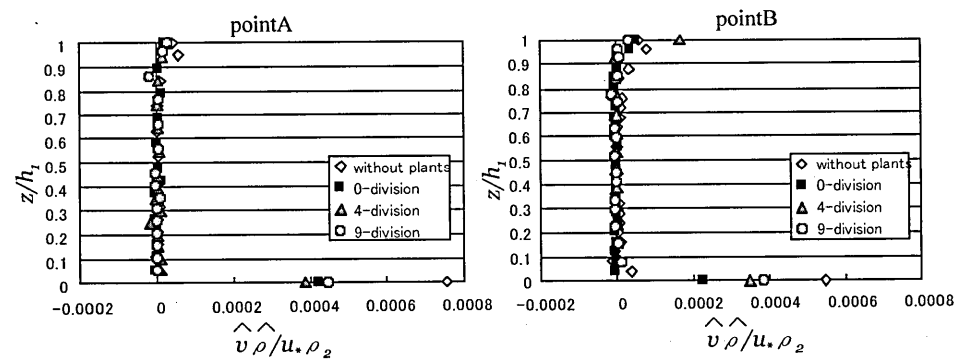


**Fig. 12.** The profiles of the density flux.

## CONCLUSION

Based on the above results, the following conclusions can be drawn:

(1) The entrainment velocity at the density interface with floating water plants was smaller than without plants. And it became large as the gregarious density of the floating water plants became small.

(2) The values of the turbulent characteristics variables of the upper layer decreased by existence of the floating water plants. However, if the gregarious density of the floating water plants became small, it increased.

(3) The scale of turbulent mixture between the upper and lower layers was less near water plants than at the center of a water body, and the influence by the difference of the gregarious density of the floating water plants appears more notably near water plants.

## ACKNOWLEDGEMENTS

The authors wish to thank Laboratory of Drainage and Water Environment, Division of Regional Environmental Science, Department of Bioproduction Environment Science, Faculty of Agriculture, Kyushu University for the convenience in the conducting the experiment.

## REFERENCES

Mori, K., Y. Tohara, S. Shikasho, K. Hiramatsu, O. Kato and Y. Cho 1989 Turbulent Structure of Two Layer Stratified Density Flow. *Transaction of the Japanese society of irrigation, drainage and reclamation engineering* (in Japanese), **144**: 75–84

Ozaki, A., R. Muramatsu, K. Mori, E. Inoue and T. Haraguchi 2002 Effect of Wind Induced Flow in a Closed Density Stratified Water Area Partially Covered with Floating Water Plants. *Jarnal of the Faculty of Agriculture, Kyushu University*, **47**: 139–147

Tsuruya, H. 1983 Experimental Study of Wind Driven Currents in a Wind–Wave Tank –Effect of Return Flow on Wind Driven Currents–. *Report of the port and harbour research institute*, **22**(2): 128–174

Wu, J. 1973 Wind–Induced Turbulent Entrainment Across a Stable Density Interface. *Journal of Fluid Mechanics*, **61**: 275–287